Behaviour of recycled aggregate concrete beam-column connections in presence of PET fibers at the joint region

Comingstarful Marthong[*]

Department of Civil Engineering, National Institute of Technology Meghalaya, Shillong 793003, India

Abstract. In this paper the behavior of reinforced concrete (RC) beam-column connections under cyclic loading was analyzed. The specimens, manufactured in a reduced-scale were made of (a) recycled aggregate concrete (RAC) by replacing 30% of natural coarse aggregate (NCA) with recycled coarse aggregate (RCA) and (b) RAC incorporating Polyethylene terephthalate (PET) fiber i.e., PET fiber-reinforced concrete (PFRC) at the joint region. PET fiber (aspect ratio=25) of 0.5% by weight of concrete used in the PFRC mix was obtained by hand cutting of post-consumer PET bottles. A reference specimen was also prepared using 100% of NCA and subjected to similar loading sequence. Comparing the results the structural behavior under cyclic loading of RAC specimens are quite similar to the reference specimens. Damage tolerance, load resisting capacity, stiffness degradation, ductility, and energy dissipation of the RAC specimens enhanced due to addition of PET fibers at the joint region. PFRC specimens also presented a lower damage indices and higher principal tensile stresses as compared to the RAC specimens. The results obtained gave experimental evidence on the feasibility of RAC for structural use. Using PET fibers as a discrete reinforcement is recommended for improving the seismic performance of RAC specimens.

Keywords: beam-column connections; recycled aggregate concrete; mechanical properties; polyethylene terephthalate fiber; cyclic loading; seismic performance

1. Introduction

Recycled aggregate has been use as a replacement of the natural aggregate (NA) for a number of years. Recycling of such waste is a beneficial from the viewpoint of environmental preservation and effective utilization of resources. Most of the past achievement on using recycled aggregate (RA) for concrete productions have been extensively reviewed and summarized by Behera *et al.* (2014). It shown that studies were mainly deal in the processing of demolished concrete, mixture design and characterizing the physical and mechanical properties as well as the durability improvement. Numerical model for predicting the compressive strength of recycled aggregate concrete (RAC) using gene expression programming (GEP) has also been developed (Abdollahzadeh *et al.* 2016). The mechanical and durability performances RAC are generally inferior to conventional concrete. The response of RAC towards mechanical action however depends upon the level of replacement by RA, water cement ratio (w/c) and the moisture condition of RA (Ajdukiewicz and Kliszczewicz 2002). Numerous experimental investigations showed that reduction in mechanical strength is not much prominent, when RA replacement is up to 30% (Rao *et al.* 2011, Hancen 1992, Xiao *et al.* 2012, Limbachiya *et al.* 2004). To improve the inferior quality of RAC, techniques such as incorporating mineral admixtures like silica fume, fly ash,

GGBS, nano silica etc. into concrete mix (Rao *et al.* 2011, Kou *et al.* 2007, Butler *et al.* 2013), impregnated RA in cement slurry (Kong *et al.* 2010), adding polymer derived from recycled polyethylene terephthalate (PET) plastic into RAC mix (Jo *et al.* 2008) and inclusion of fibers derived from post-consumer PET bottles (Marthong and Marthong 2015) etc. has been tried and found effective. Further, results reported by various researchers (Padmini *et al.* 2009, Tabsh and Abdelfatah 2009, Corinaldesi 2010), showed that RAC exhibited a similar behavior, which can be adequately used in concrete technology application. For confident utilization of RAC in the construction industry, the structural behavior of recycled concrete ought to be investigated. Some past studies concerning the behavior of beams (Han *et al.* 2001), columns (Chao *et al.* 2010) and beam-column joints (Corinaldesi and Moriconi 2006, Corinaldesi *et al.* 2011, Viviana *et al.* 2014), reinforced concrete (RC) frame structure (Xiao *et al.* 2006) prepared from RAC are reported. Most of their findings on their structural behavior are positive, which reveal that cracking pattern and failure modes of the reinforced recycled aggregate concrete (RRAC) are quite similar to the conventional RC. However, due to the early cracking of the concrete matrix the load carrying capacity of the RRAC is reduced but to an allowable extent.

The behavior of RC beam-column connection plays an important role in the response of a framed structure. It is the weakest link of the frame structures (Matheus and Vladimir, 2016). However, it strongly influences the seismic behavior and energy dissipation capacities of the moment resisting frames. From the past devastating earthquake among the different configurations the exterior connections which is

---

*Corresponding author, Associate Professor
E-mail: commarthong@nitm.ac.in

confined by only two or three framing beams and having lesser confinement level had suffered more in comparison to the interior ones. The building codes recommend the minimum amount of longitudinal and transverse reinforcement (IS 13920 1993, ACI 318-08 2008) and use of closely spaced hoops as transverse reinforcement (ACI-ASCE Joint Committee 352 1976) at the beam-column connections in order to achieve a better seismic performance. The practical difficulties during construction due to these congested joint regions may lead to a honey combing in concrete (Kumar *et al.* 1991). Reducing the hoops spacing of a transverse reinforcement may also lead to improper bonding between the reinforcing bars and the concrete and thus achieving a proper concrete confinement level within the joint regions may not be possible. Conventional methods such as strengthening the joints region with fiber-reinforced polymer (FRP) (Ghobarah and Said 2002, Karayannis and Sirkelis 2008), concrete Jacketing (Karayannis *et al.* 2008) and steel jacketing (Hadi and Tran 2014), Sasmal *et al.* 2010) etc. and rehabilitating the damaged structures using epoxy resin injection (Marthong *et al.* 2013) is an effective way of improving the seismic capacity of the beam-column connections. While, the mentioned methods mostly used for strengthening and rehabilitating the existing RC beam-column connections. For a new construction the use of fiber-reinforced concrete (FRC) found to be an effective technique for compensating the reinforcement detailing requirements at the joint region. Experimental study (Bayasi and Gebman 2002) proved the confinement effect of using FRC in the joint region for reducing the lateral reinforcement. Studies (Oinam *et al.* 2014, Dhaval *et al.* 2015) show that addition of randomly oriented discontinuous steel fibers into the joint region of RC beam-column connections significantly improves the damage tolerance, lateral load resisting capacity, ductility, toughness and slower the degradation rate in stiffness. In substitution of steel fiber polymeric fibers made of nylon, aramid, polypropylene, polyethylene and polyester has been used as concrete reinforcing materials. Various experimental studies (Panyakapo and Panyakapo 2007, Fraternali *et al.* 2011, Foti 2013, Marthong and Sarma 2016, Kim *et al.* 2010, Foti 2011, Pereira de Oliveira and Castro-Gomes 2011, Fraternali *et al.* 2013) showed PET fiber has a potential use for enhancing the mechanical properties of concrete that can replace steel fiber. The fiber content generally varies from 0.1% to 1.0%. However, a fiber content of 0.5% by weight of concrete is reported as an optimum percentage (Marthong 2015). Seismic parameters such as load resisting capacity, ductility, energy dissipation capacity and stiffness of beam-column connection improve when a concrete mix incorporating PET fiber is use at the joint region (Marthong and Marthong 2016).

Due to the inferior quality of RA use for concrete production, the seismic performance of RAC beam-column connections may be lower than those of conventional concrete. Like the conventional concrete, various techniques may be employed for improving the mechanical properties of RAC concrete. One such technique on a particularly use of PET fibers for enhancing the mechanical strength and energy dissipation capacity of RAC has been reported (Jo *et al.* 2008). The study reveals that a significant enhancement in tensile, flexural and energy dissipation capacity was achieved. Also, PET fiber has a potential for arresting crack formation due to fiber-bridging action inside the concrete matrix. Thus, it is expected that use of PET fiber in the joint region of RAC beam-column connections also would delay the crack formation and crack growth. This would result in enhancement of displacement ductility of the beam-column connections due to delayed bond failure.

The novelty of this research respect to similar studies on using steel fibers (Dhaval *et al.* 2015) and PET fibers (Marthong and Marthong 2016) at the D-region of the beam-column connections for improving the seismic performance is, principally, that PET fiber with aspect ratio (length/width) of 25 has been utilized in RAC beam-column connections, not found in previous authors. The fibers were manually cut from the post-consumer PET bottles and mix with concrete at fiber content of 0.5% by weight of concrete. RAC specimens shown in Table 1 was characterized from mechanical point of view, and RAC structural behavior was tested by mean of reduced-scale exterior RC beam-column connections under cyclic loading to test their ability in improving their damage tolerance, load resisting capacity, stiffness degradation, ductility, and energy dissipation capacity with the addition of PET fibers to RAC concrete mix. The specimens, manufactured in a reduced-scale were prepared of RAC and addition of PET fibers at the joint region i.e PET fiber reinforced concrete (PFRC). RAC specimens were prepared by replacing 30% of NCA with RCA. A reference specimen (Marthong and Marthong 2016), which was casted using NA, was used herein to compare the behavior of RAC. Damage indices and nominal principal tensile stresses in beam-column joint region (damaged regions) of beam-column specimens were also evaluated for better understanding of their behavior.

2. Experimental program

The testing program consisted of two parts:
1. Tests to evaluate the mechanical properties using 30% RCA as partial replacement of NCA and their enhancement due to the addition of PET fibers in RAC concrete.
2. To study the behavior of exterior reinforced RAC beam-column connections due to the addition of PFRC at the D-region.

2.1 Materials

Ordinary Portland Cement (OPC) of 53 grades conforming to IS: 12269 (1987) was considered. The maximum size of NCA's was 16 mm. River sand was used as fine aggregate (0-4.75 mm size). The RCA's (5-16 mm size) are obtained from the demolished reinforced cement concrete (RCC) roof slab 20 years old and the properties of the old concrete are unknown. The large pieces of the roof slab are transported to the laboratory and broken into pieces of aggregates smaller than 20 mm in size and sieved through a 16 mm sieve. The aggregates greater than 16 mm in size are further broken to a maximum size of 16 mm and

Table 1 Specimen for evaluating the mechanical properties of concrete

Mixes	Cube (mm)	Cylindrical (mm)	Prism (mm)	Fiber contents (%)	Total mixture
M-0	150x150x150	150x300	500x125x125	0	100 % NCA
M-30	150x150x150	150x300	500x125x125	0	70 % NCA + 30 % RCA
M-30/0.5	150x150x150	150x300	500x125x125	0.5	70 % NCA + 30 % RCA+ 0.5% PET fiber
Test parameter	Compressive strength	Splitting tensile strength	Flexural strength		

Table 2 Physical properties of NCA and RCA

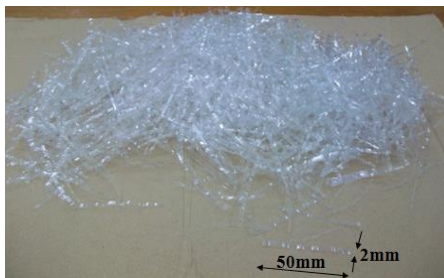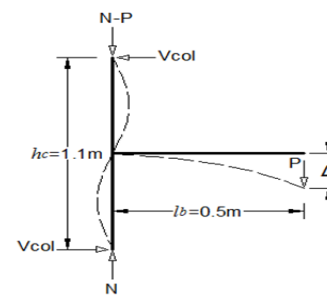| Sample	Apparent density (kg/m^3)	Bulk density (kg/m^3)	Grading (mm)	Elongated particle content (%)	Saturated surface dry absorption (%)	Water absorption (%)	Crush index (%)
NCA	2830	1560	5-16	5	1.55	4.05	5.8
RCA	2400	1230	5-16	10	7.60	9.30	9.8

Fig. 1 Straight slit sheet fiber of PET

Fig. 2 Isolated exterior beam-column connection

then both the materials are mixed and sieved again. Aggregates used have been tested as per relevant codes (IS 2386a 1963, IS 2386b 1963) and the physical properties are presented in Table 2. The polymeric fiber type use for enhancing the mechanical properties of RAC was PET fiber. The geometry of PET fiber considered was "straight slit sheet", which has the shape similar to those of steel fibers (ACI Committee 544 1996). Fig. 1 shows the geometry of fiber use in this study, which were produced by hand cutting from post-consumer PET bottle of 1 l capacity. The length of fiber is 50 mm, width is 2 mm and thickness is 0.5 mm with an aspect ratio (length/width) of 25. The specific gravity and tensile strength of PET fibers is found out to be 1.38 and 155 MPa respectively.

2.2 Concrete mixture proportions

Table 1 presented the specimens and test parameters for characterizing the mechanical properties of concrete, three types of concrete mixes were considered (i) M-0 were prepared using 100% of NCA (ii) 30% of NCA were replaced by RCA for preparing mix M-30 (iii) M-30/0.5 is similar to M-30 except with an inclusion of PET fibers. All concrete mixes were prepared with the same w/c of 0.5 and the same degree of workability (slump value of 60 mm), evaluated according to IS 1199 (1959). The concrete mixes were designed for a characteristic cube compressive strength of 25 MPa which resulted in a target mean cube compressive strength of 31.6 MPa as per IS 10262 (2009). The concrete mixes were produced with 372 kg/m^3 of cement, 733 kg/m^3 of fine aggregate, 1087 kg/m^3 of NCA and 326 kg/m^3 of RCA for a w/c of 0.5 and a compaction factor of 0.9. The amount of PET fibers added was 0.5% by
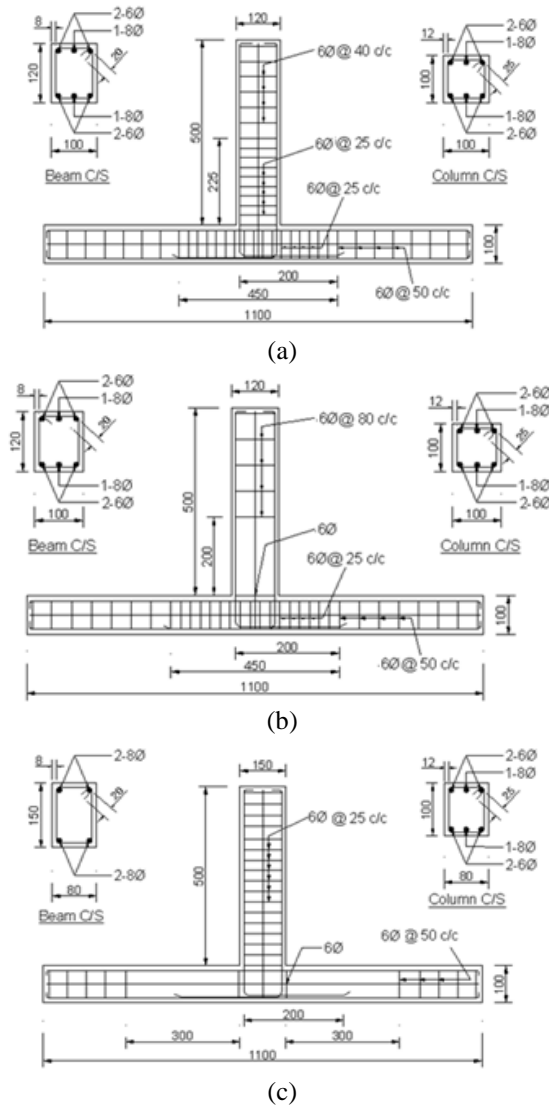
weight of a total concrete mixture. To achieve a better workability, 0.5% and 0.6% of superplasticizer by volume of water was used in the mixing of M-30 and M-30/0.5 respectively. In each sample three specimens were cast. Concrete containing no fiber was use as a reference specimen (M-0). Specimens from the mould were removed after 24 hours of casting and were kept in a water tank for 28 days curing before testing.

2.3 Selection of RC beam-column connections

A free body diagram of an isolated exterior beam-column connection in its deformed position is shown in Fig. 2. It comprises of half height of a column at top and bottom as well as half of a beam length, which corresponded to the points of contra-flexure in beam and column under lateral loads. In this figure, h_c is the story height, l_b is half beam span corresponding to the length of the beam connected to the selected joint, N is the internal axial force of the column, P is the beam-tip load, V_{col} *is* the column shear force and Δ is the vertical beam-tip displacement. It may be noted that the symmetric boundary condition were maintained at both the ends of column for isolation of a single unit of beam-column connection. In this study, a typical full scale residential building with floor to floor height of 3.3 meters and the beam effective span of 3.0 meters were considered. The connection was scaled down to one-third size for experimental investigation.

2.4 Description of RC beam-column connections

The present study considered three typical deficiency

(a)

(b)

(c)

Note: all dimensions are in mm

Fig. 3 Reinforcement detailing of specimens (a) BWF (b) BWS and (c) CWS

namely, (a) beam-column connections with beam weak in flexure (BWF), (b) beam-column connections with beam weak in shear (BWS) and (c) beam-column connections with column weak in shear (CWS). Fig. 3 presented the reinforcement detailing of all the specimens. The longitudinal reinforcement consisted of high yield strength deformed (HYSD) bar of 8 mm diameter (Fe 500). A mild steel (MS) bar of 6 mm diameter (Fe 250) was also used as longitudinal as well as transverse reinforcement. The yield stress (MPa) and ultimate stress (MPa) for HYSD bars tested as per code provisions (IS 432 I 1982, IS 1608 1995) were found out to be 530 MPa and 620 MPa, while the same for Fe 250 bars were 285 MPa and 450 MPa respectively.

The detailing of BWF specimen is shown in Fig. 3(a). Following the standard code of practice (IS 13920 1993, IS 456 2000) the beam specimen was designed as under reinforced section. A cross section of 100 mm×100 mm and 100 mm×120 mm for column and beam elements

respectively was considered. HYSD bars of 8 mm diameter and MS bar of 6 mm diameter were used as main bars in both column and beam. Following the code provision IS 13920 (1993) a lateral tie of 6 mm diameter MS bar at 25 mm c/c spacing was used in the special confinement zone of the column, while the remaining part was increased to 50 mm c/c. The shear reinforcement used in beam was of 6 mm diameter MS bar having spacing of 25 mm c/c near the beam-column joint for a length of 225 mm and a spacing of 40 mm c/c was provided in the remaining part.

The detailing of BWS specimens is shown in Fig. 3(b). Under this category, the specimen was exactly similar in all respect to that of BWF specimen, except the shear reinforcement provided in beams. The amounts of shear reinforcements were reduced to make the beam weak in shear. To reduce the shear reinforcements in beam, lateral ties with 6 mm diameter bars with a spacing of 80 mm c/c were provided as shear reinforcement. To maintain the pre-defined failure location in the beam only the first two stirrups with a wider spacing of 200 mm c/c near the joint was placed.

Strong beam-weak column principle was followed for design of CWS specimen. The cross section of column as shown in Fig. 3(c) was kept same as that of BWF and BWS specimens, while the cross section of a beam was increased to 80 mm×150 mm. The main reinforcements in column were maintained similar to those of earlier cases, while same was increased in beam. In order to ensure the shear weakness of these specimens a wider lateral ties spacing of 300 mm c/c on either side of the joint region was provided. In the remaining part the spacing of lateral ties was reduced to 50 mm c/c. The detailed descriptions of all specimens are given in Table 3.

2.5 Casting of RC beam-column connections

Three sets of exterior RC beam-column connections were cast. Each set consisted of three types of specimens namely BWF, BWS and CWS. The first sets of specimens (Marthong and Marthong 2016), which was casted using an ordinary concrete (100% of NCA) were treated as reference specimens (NAC) and named as BWF/$_{NAC}$, BWS/$_{NAC}$ and CWS/$_{NAC}$. Keeping the geometric dimensions, grade of concrete and steel, the amount and detailing of reinforcing bars constant as those of the respective reference specimens. The second set of specimens were cast by replacing 30% of NCA in an ordinary concrete by RCA and were named as BWF/$_{RAC}$, BWS/$_{RAC}$ and CWS/$_{RAC}$ respectively. Keeping the same mixes and replacement level as those of the second set, the third set of specimens were cast with the addition of PFRC mix at the D-region (ACI Committee 318-08 2008) of the beam-column connections (PFRC mix consisted of 70 % NCA+30 % RCA+0.5% PET fibers) and were named accordingly e.g., BWF/$_{PFRC}$, BWS/$_{PFRC}$ and CWS/$_{PFRC}$ respectively. Fig. 4(a) show one set of cast specimens. The D-region of the connections as shown in Fig. 4(b) denotes the locations where PFRC mix were used in the third sets of specimens. All specimens were cast with a concrete mix which has a mean cube compressive strength of not less than 31.6 MPa.

Table 3 Descriptions of RC beam-column connections

Specimen	Beam			Column		
	Span (mm)	Section (mm×mm)	Longitudinal Reinforcement	Length (mm)	Section (mm×mm)	Longitudinal Reinforcement
BWF & BWS[b]	500	100×120	1-8ϕ+2-6ϕ-top 1-8ϕ+2-6ϕ-bottom	1100	100×100	2-8ϕ+4-6ϕ
CWS	500	80×150	2-8ϕ-top 2-8ϕ-bottom	1100	100×100	2-8ϕ+4-6ϕ

[b]Beam weak in shear specimens have same dimensions and longitudinal reinforcement as that of beam weak in flexure specimens except the shear reinforcement provided in beam.
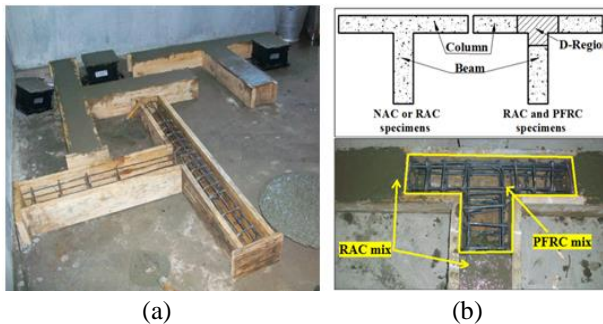

(a) (b)
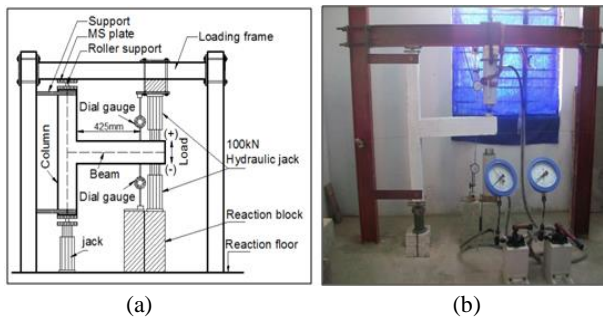
Fig. 4 (a) Set of cast specimens and (b) D-region for PFRC mix

(a) (b)

Fig. 5 Testing of beam-column connection (a) Test set-up (b) Actual testing arrangement

Fig. 6 Loading history

2.7 Loading sequence

The loading sequence suggested by Vidjeapriya and Jaya (2013) is adopted in the present study. However, one loading cycle at every amplitude of displacement was considered instead of three cycles. The loading history is presented in Fig. 6. The drift angle is defined as the ratio of beam tip displacement to the length of the beam measured from the joint to the position of the dial gauge. Drift obtained by horizontally displacing the beam ends are equivalent to the inter storey drift angle of a frame structure subjected to lateral loads. The two hydraulic jacks mounted on top and bottom of the beam tip end were used to apply the reversed cyclic loading. As suggested by Ghobarah *et al.* (1997) an axial load of 10% of gross capacity of column was applied to the column end by using a hydraulic jack to represent the dead load transferred from upper floors.

3. Behavior of recycled aggregate concrete: results and discussion

At a constant w/c of 0.5, the workability measured as per code provision (IS 1199 1959) for M-30 concrete reduces about 15% in comparison to M-0 concrete. The additions of 0.5% PET fiber to M-30 concrete mix further drops down the workability to 20%. The high absorption of free water from the mixture during mixing process, which cause high water demand of the mix and fibers not able to envelop perfectly by concrete may be the reasons for these behavior. This shows that RAC concrete (M-30 and M-30/0.5) results in a significant effect on the workability of concrete. Same level of workability as those of mix M-0 could be achieved by adding superplastisizer of 0.5% and 0.6 % by volume of water concrete respectively.

The concrete specimen as presented in Table1 was used for evaluating the mechanical properties. Test parameters

2.6 Test set-up and instrumentation

Schematic diagram of the test set-up and the actual testing arrangement is shown in Fig. 5. A loading frame of 1000 kN capacity and hydraulic jack of 100 kN was used for applying the load to the specimens. In the testing frame, the column was placed in the vertical position while the beam was placed in horizontal position. An axial load using hydraulic jack was applied to the column to represent the gravity load. To model the actual conditions where the moments were approximately zero at the mid-span of the column when subjected to lateral loading a roller supports were provided at both ends of the column. The cyclic loading was applied manually at a distance of 100 mm from the free end of the beam by mean of two hydraulic jack mounted at top and at bottom. The hydraulic jack of 100 kN capacity was equipped with an in-built manually operated pumping units fitted with bourdon tube type load gauge and high pressure flexible hose pipe. Two dial gauges of 100 mm measuring range were placed at top and bottom face of the beam tip to measure the vertical displacement of the beam.
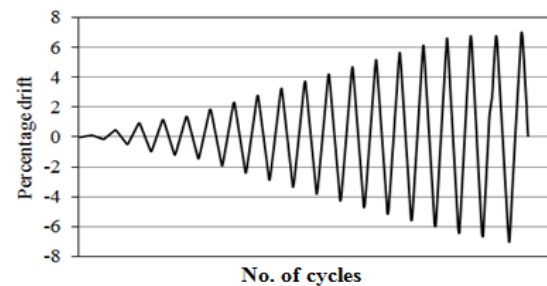
Table 4 Strength and energy absorption of concrete specimens

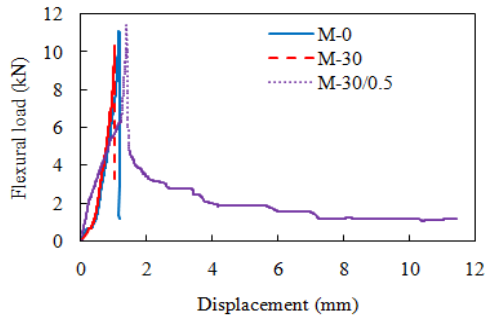| Concrete Mix	Compressive strength (MPa)	Tensile strength (MPa)	Flexural strength (MPa)	Energy absorption (kN-mm)
M-0	34.56	3.68	3.75	5.32
M-30	33.78	3.31	3.39	4.87
M-30/0.5	31.82	4.15	4.33	15.78

Fig. 7 Load versus displacement plot of concrete prism

included are compressive strength, splitting tensile strength and flexural strength test. The results of compressive strength test carried out as per code provision (IS 519 1959) are presented in Table 4. The results indicated a slight reduction in compressive strength (generally -2%) at 30% replacement level and further reduced to about 8% due to the addition of PET fibers as compared to reference specimens. The splitting tensile strength of M-0 and M-30 concrete tested in accordance to code provision (IS 5816 1999) is presented in Table 4. They showed slight lower tensile strength (-10%). However, due to good dispersion of fibers which resulted in a better bridging action in a concrete matrix, M-30/0.5 concrete specimen showed improvement over M-0 and M-30 concrete about 11% and 20% respectively. M-0 and M-30 specimens suddenly split into two parts under compressive load, while M-30/0.5 concrete specimen exhibited cracking but did not fully separate. This suggests that RAC incorporating PET fiber has the ability to dissipate more energy.

The flexural strength of prismatic specimens was evaluated as per code provision (IS 519 1959) is present in Table 4. M-30 specimens presented a slightly lower strength (-10%) as compared to M-0 specimen. However, with the existence of PET fibers, external load can be transferred to the fibers through the interfacial bonding between the fibers and concrete matrix as a result, the flexural toughness of M-30/0.5 specimens increased by 15%. It is evident from the load versus displacement curves shown in Fig. 7 that M-0 and M-30 concrete specimens failed suddenly with a lower displacement level as compared to M-30/0.5. Further, the ability of a structural element to resist an earthquake load depends to a large extent on its capacity to dissipate its energy. The energy dissipation capacity, which is represented by the area under the load versus displacement curves (Shannag and Ziyyad 2007) and presented in Table 4 also reveal that the addition of PET fibers in a concrete mix reflects a better energy dissipation capability of the specimens.

Fig. 8 Failure modes of BWF specimens

4. Behavior of RC beam-column connections: results and discussion

4.1 Failure mode of specimens

Figs. 8 to 10 presented the failure modes of specimens due to cyclic loading. It is observed that the initial cracks in all the beam-column connections mainly developed at the joint interface. With further application of cyclic loads, the cracks propagated toward their weakest shear zone or the flexural zone or widening up the initial cracks at the joint face and a maximum crack width of 5 mm was observed. Under cyclic loading the RAC specimens shows a brittle mode of failure with wider crack compared to NAC specimens. Due to the early fragmentation of the concrete matrix, RAC specimens also presented a lower load carrying capacity. However, the PFRC specimens presented more closely spaced crack and the width of such cracks was smaller than those of the NAC and RAC specimens. Also, due to the delayed in the fragmentation of the concrete matrix, the PFRC specimens can undergo moredisplacement level and presented slightly higher ultimate loads carrying capacity as compared to RAC specimens. This shows that addition of PET fiber at the D-region of the beam-column connections reduces the damage level in the specimen due to the fiber-bridging action and hence PFRC specimens are capable of taking higher loads.

As observed in Fig. 8, all BWF specimens experienced maximum moment at the joint region and the initial crack also appeared there. The formation of a joint hinge was observed to delay for BWF/$_{PFRC}$ specimen as compared to other two due to the presence of fibers at the D-region, which offered more crack resistance during cyclic loading. The faster growth of cracks for BWF/$_{RAC}$ specimen, which spreads away from the joint region, reveals a brittle mode of failure in comparison to BWF/$_{PFRC}$ specimen.

It may be observed from Fig. 3(b) that the shear weakness in the beam for BWS specimens is over a length of 200 mm from the column interface. Thus, shear cracks are likely to occur over this length, where the Shear force is constant. Examination of all the BWS specimens (Fig. 9) at the end of the experiment revealed the existence of visible shear cracks within the weak shear zone as
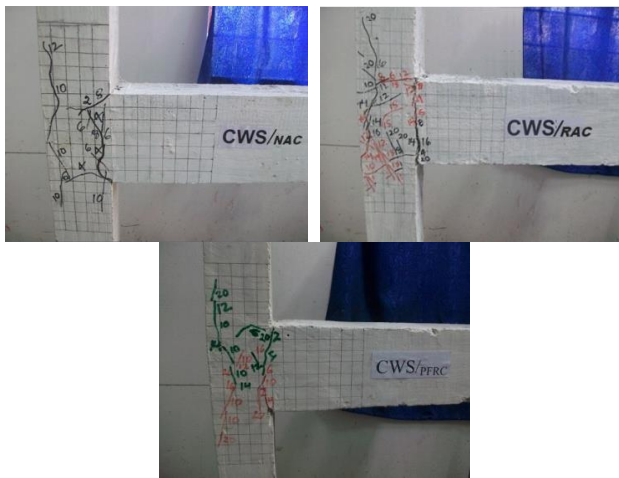
Fig. 9 Failure modes of BWS specimens

Fig. 10 Failure modes of CWS specimens

Fig. 11 Hysteretic responses

expected. BWS/$_{RAC}$ and BWS/$_{PFRC}$ specimens fail in a similar pattern with cracks not only concentrating on the weakest shear zone but also propagating towards the joint regions. A numbers of smaller cracks were distributed at weakest shear zone and at the joint region for BWS/$_{PFRC}$ specimens indicating the fiber-bridging action in the specimens, which improve the damage resistance under reversed cyclic loading compared to BWS/$_{RAC}$ specimen.

Further, the damage states of CWS specimens at the end of the test are shown in Fig. 10. Since the beam is much stronger than the column, cracks initiating from the joint region are propagating towards the weakest shear zone in the column, while the beam parts remain undamaged. The failure patterns of the specimens were as expected by the built-in deficiencies in the specimens as considered during the design. However, CWS/$_{RAC}$ and CWS/$_{PFRC}$ specimens presented a different failure pattern in comparison to CWS/$_{NAC}$ specimen. More cracks at the joint region and at the column part for CWS/$_{RAC}$ and CWS/$_{PFRC}$ specimens were observed, which indicate the brittleness of the specimens. Closely observing the cracks growth towards the weakest shear zone for CWS/$_{PFRC}$ specimen it is observed to be delayed as compared to CWS/$_{NAC}$ specimen. This shows the ability of PET fibers to prevent the cracks formation and thus make the specimens to undertake more tensile strength
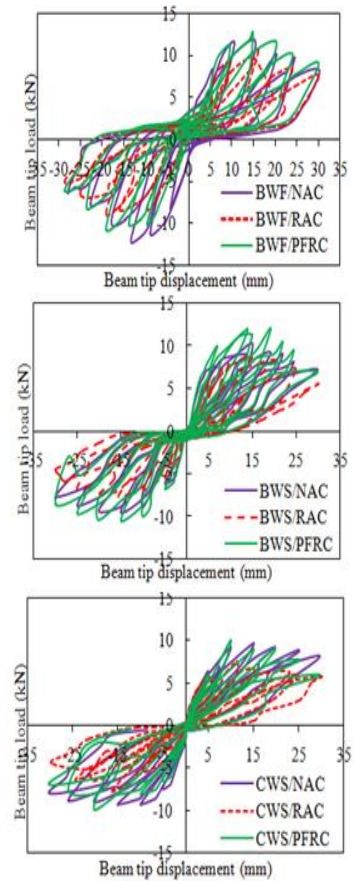
during cyclic loading.

Overall, it can be accomplished that the beam-column connections made of RA cause multiple cracking under cyclic loading as compared to the NAC specimens, indicating the brittleness of the specimens. However, their failure patterns are quite similar to the reference specimens. An RAC beam-column specimen loses its resistance completely after cracking. Whereas, PFRC specimens can sustain a portion of its resistance following cracking to resist more cycles and produces ductility in the material.

4.2 Hysteretic response of specimens

The hysteretic response obtained by plotting the test data is presented in Fig. 11. Various seismic parameters such as ultimate strength, energy dissipation, stiffness degradations and ductility of the specimens were evaluated from these hysteretic responses. Capacity comparison of specimens is presented in Table 5. The behaviors of these connections were studied by comparing these parameters. RAC beam-column connections exhibited similar responses as compared to the reference specimens. However, PFRC beam-column connections offered more resistance to cracking compare to RAC specimens. The ductile property imparted by PET fiber presence at the D-region makes the specimens capable of taking higher loads. This shows that, incorporation PET fibers into the concrete mix enhanced the lateral load carrying capacity of RAC beam-column connections.
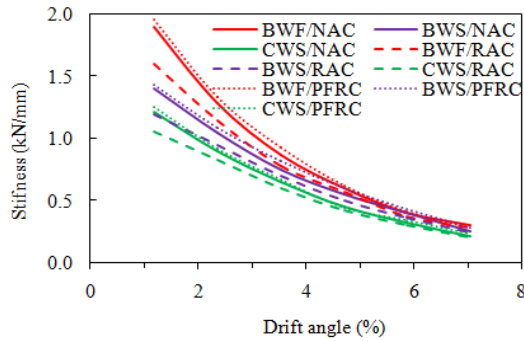
Fig. 12 Comparison of degradation of stiffness degradation of the test specimens

Fig. 13 Cumulative energy dissipation of beam-column specimens

4.2.1 Stiffness degradation

Secant stiffness is evaluated as the peak-to-peak stiffness of the beam tip load-displacement relationship. The secant stiffness is an index of the response of the specimen during a cycle and its strength degradation from a cycle to the following cycle. It is calculated as the slope of the line joining the peak of positive and negative capacity at a given cycle. The slope of this straight line is the stiffness of the assemblage corresponding to that particular amplitude (Naeim and Kelly 1999). The stiffness degradation of the test specimens is presented in Fig. 12. Irrespective of the deficiency types, they showed a similar degradation trends. The reduction in stiffness for NAC is about 13% to 16%. However, due to fiber-bridging actions, which control the early cracking of the specimens PFRC specimens exhibited equal or marginally higher in stiffness as compared to the NAC beam-column connection. Evaluating the reduction in stiffness of all specimens it was observed that the degradation rate of stiffness is slightly lower for PFRC specimens at the same displacement level. The lower degradation of stiffness is a desirable property in earthquake like situations. It was observed during the past earthquake that most of the RC structures failed due to sudden loss of stiffness with increasing lateral movement.
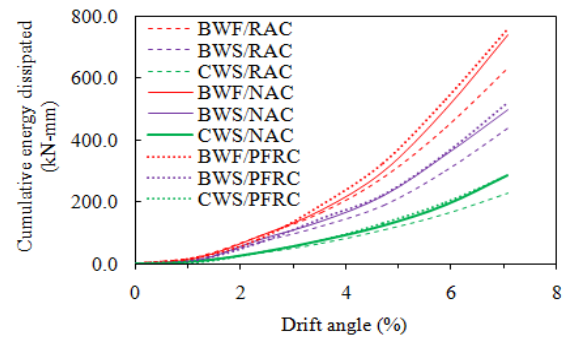
Therefore, from these comparisons it can be concluded that inclusion of PET fibers to RAC mix lead to an enhancement of stiffness of RAC beam-column connections.

4.2.2 Cumulative energy dissipation

The performance of a structural element during seismic excitation depends to a large extent on its capacity to dissipate energy. The area of hysteresis loop is a measure of the energy dissipated. The cumulative energy dissipated at particular amplitude was calculated by summing up the energy dissipated in all the preceding cycles including that amplitude. The energy dissipation of specimens is presented in Table 5 and percentage gain/reduction in Table 6; all RAC specimens presented the lowest energy dissipation capacity. The increase in energy dissipation of PFRC specimens shows PET fiber has a tremendous potential use in beam-column connections in seismic zones for enhancement of ductility behavior. Further, Fig. 13 compares the plots of cumulative energy dissipation versus drift angle of all sets of specimens. The PFRC beam-column connections showed equal or marginal enhancement in energy dissipation capacity as compared to those of the reference specimen. The increase in stiffness at the end of imposed displacement history attracted more load

Table 5 Capacity comparisons of RC beam-column connections

Specimens	NAC (Marthong and Marthong 2016)			RAC			PFRC		
	Average load capacity, kN (+ve and -ve)	Energy dissipation (kN-mm)	Ductility (d_u /d_y)	Average load capacity, kN (+ve and -ve)	Energy dissipation (kN-m)	Ductility (d_u /d_y)	Average load capacity, kN (+ve and -ve)	Energy dissipation (kN-m)	Ductility (d_u /d_y)
BWF	12.00	631.80	3.52	9.96	601.80	2.73	11.86	629.45	3.55
BWS	10.15	440.97	3.04	9.24	330.12	2.25	9.87	389.51	2.96
CWS	9.25	250.19	2.61	7.23	205.17	1.55	9.69	245.45	2.72

Table 6 Percentage gain/reduction with respect to control specimens (Marthong and Marthong 2016)

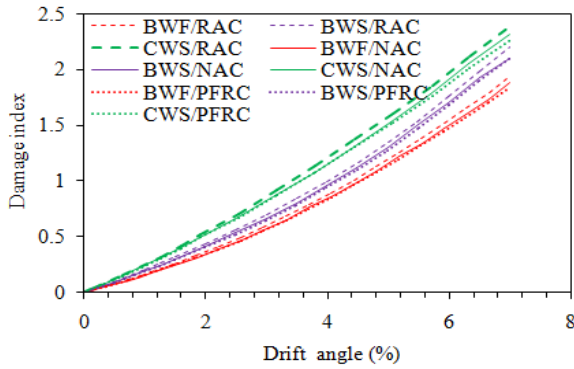| Specimens	RAC			PFRC		
	Load capacity	Energy dissipation	Ductility	Load capacity	Energy dissipation	Ductility
	Percentage gain (+) /reduction (-)	Percentage gain (+) /reduction (-)	Percentage gain (+) /reduction (-)	Percentage gain (+) /reduction (-)	Percentage gain (+) /reduction (-)	Percentage gain (+) /reduction (-)
BWF	-17	-4.75	-22.44	-1.17	-0.37	0.85
BWS	-8.97	-25.14	-25.99	-2.76	-11.67	-2.63
CWS	-21.84	-17.99	-40.61	4.76	-1.89	4.21

Fig. 14 Comparison of damage indices of the tested specimens

corresponding to any drift angle due to fiber-bridging actions for PFRC specimens as compared to those RAC beam-column connections, which prevent the initial crack propagations. Thus, the total area enclosed by the plot of beam tip load versus beam tip displacement was more for PFRC beam-column connections. This was perhaps the reason for improvement in cumulative energy dissipation in the subsequent loading cycles.
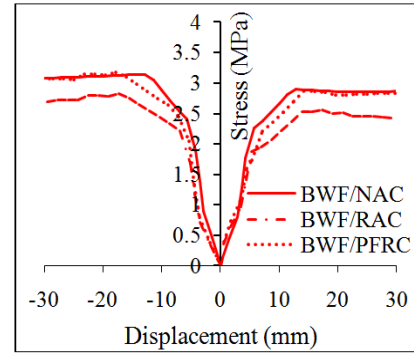
4.2.3 Displacement ductility

The displacement ductility, which is the ratio between the ultimate displacements (d_u) to the displacement at first yield (d_y) was calculated for all the specimens following the method used by Shannag *et al.* (2005) and presented in Table 5 and percentage gain/reduction in Table 6. The displacement ductility attained by RAC beam-column connections without addition of PET fibers at the joint region was found to be lower than those of the corresponding reference specimens. The displacement ductility however improved in PFRC specimens. The ability of PET fiber for arresting the macro cracking during cyclic loading leads to an enhancement of displacement ductility.
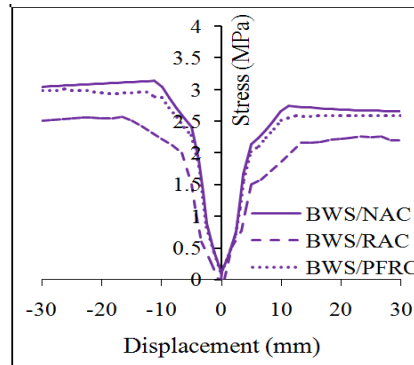
4.3 Seismic damage index

Damage indices are intended to be used as numerical indicators of damage of any structural element under any loading type. Parameters such as strain, displacement, strength, energy and intrinsic dynamic properties are used to calculate these damage indices. Damage index model of Park and Ang (1985) given in Eq. (1) was employ in this study to evaluate the damage level of the specimens.

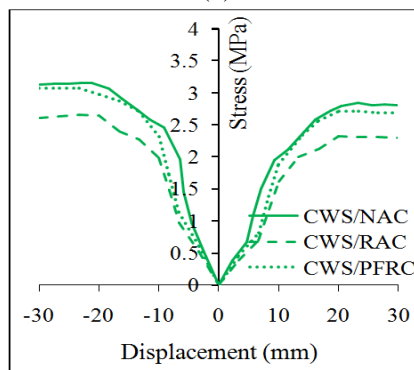$$DI = \frac{\delta_m}{\delta_u} + \frac{\beta}{\delta_u Q_y} \int dE \qquad (1)$$

where δ_m the maximum deflection attained during seismic loading, δ_u is the ultimate deflection capacity under monotonic load, Q_y is the yield force, dE is the incremental dissipated hysteretic energy and β is the strength degradation parameters. Parameters involved in the evaluation of the damage index were estimated as per Karayannis *et al.* (2008). The calculated damage indices for all specimens based on the above model are presented in Fig. 14. These figures show that the damage indices

(a)

(b)

(c)

Fig. 15 Nominal principal tensile stress developed in beam-column joint region (a) BWF (b) BWS and (c) CWS specimens

increase as the damage of specimens grow further with increased drift values. Further, all the curves of the damage indices are nearly linear, which suggest that the growth of damages in different specimens were stable. Further, due to early fragmentation of concrete matrix, all RAC beam-column connections presented a higher damage index. However, with the inclusion of PET fiber, a lower damage index is observed for all PFRC beam-column connections. Thus the lower damage index presented by PFRC specimens indicated a significant contribution of PET fibers for improving the seismic capacity of these connections.

4.4 Nominal principal tensile stresses

To have a better understanding of their behavior, nominal principal tensile stresses in beam-column joint

region (damaged regions) were evaluated and compared in Fig. 15. From this figure it is can be deduced that the developed nominal principal tensile stresses of all RAC beam-column connections are much lower than those of the reference specimens. However, the ability of PET fibers to prevent the early cracking and arrest the crack growth during cyclic loading; all PFRC beam-column connections showed substantial increased in the nominal principal tensile stresses.

5. Conclusions

The suitability of RCA as partial replacement of NCA in the production of concrete mix and the technique for enhancement their mechanical properties using PET fiber is investigated.

By comparing the results of M-0 and M-30 concrete mix, almost the same mechanical strength can be achieved. In particular, almost the same level of compressive strength, lower splitting tensile strength, flexural strength (generally -10%) are found for concrete with M-30. On the other hand, due to good dispersion of PET fiber which resulted in a better bridging action in a concrete matrix, M-30/0.5 specimens showed significant improvement in the splitting tensile strength (25% more), flexural strength (27% more) and 3 times increased in energy dissipation of the concrete specimens.

In addition, on the basis of the results obtained through cyclic loading test of beam-column connections, the failure pattern of RAC beam-column connection behave similar to those of the reference specimens (NAC), which fails as per the design preferences. Important parameters related to seismic capacity such as strength, stiffness degradation, energy dissipation, and ductility were also evaluated. The RAC beam-column connections showed adequate behavior. Inclusion of PET fibers at the D-region presented a lower damage indices and higher principal tensile stresses and further enhanced the seismic capacity of the RAC beam-column connections comparable or marginally higher than those of the reference specimens.

It can be concluded from this investigation that the experimental results obtained gave evidence on the feasibility of RAC for structural uses. Used of PET fibers as a discrete reinforcement is recommended for improving the seismic performance of RAC concrete beam-column connections.

Acknowledgments

References

Abdollahzadeh, G., Jahani, E. and Kashir, Z. (2016), "Predicting of compressive strength of recycled aggregate concrete by genetic programming", *Comput. Concrete*, **18**(2), 155-163.

ACI-ASCE Joint Committee 352 (1976), "Recommendation for design of beam-column joints in monolithic reinforced concrete structures", *J. Am. Concrete Inst. Proc.*, **73**(7), 375-393.

ACI Committee 318-08 (2008), Building Code Requirements for Structural Concrete (ACI 318-08) and Commentary (ACI 318R-08), American Concrete Institute, Farmington Hills, MI.

ACI Committee 544 (1996), State-of-the-art Feport on Fiber Reinforced Concrete, ACI 544.1R-96, Re-approved 2002, American Concrete Institute, Farmington Hills, Michigan.

Ajdukiewicz, A. and Kliszczewicz, A. (2002), "Influence of recycled aggregates on mechanical properties of HS/HPC", *Cement Concrete Compos.*, **2**, 269-79.

Bayasi, Z. and Gebman, M. (2002), "Reduction of lateral reinforcement in seismic beam-column connection via application of steel fibers", *ACI Struct. J.*, **99**(6), 772-780.

Behera, M., Bhattacharyya, S.K., Minocha, A.K., Deoliya, R. and Maiti, S. (2014), "Recycled aggregate from C&D waste & its use in concrete-A breakthrough towards sustainability in construction sector: A review", *Constr. Build. Mater.*, **68**, 501-516.

Butler, L., West, J.S. and Tighe, S.L. (2013), "Effect of recycled concrete coarse aggregate from multiple sources on the hardened properties of concrete with equivalent compressive strength', *Constr. Build. Mater.*, **47**, 1292-1301.

Chao, L., Guoliang, B., Letian, W., and Zonggang, Q. (2010), "Experimental Study on the Compression Behavior of Recycled Concrete Columns", *Proceedings of the international RILEM conference on the Waste Engineering and Management*, 614-621.

Corinaldesi, V. (2010), "Mechanical and elastic behavior of concretes made of recycled concrete coarse aggregates", *Constr. Build. Mater.*, **24**(9), 1616-1620.

Corinaldesi, V. and Moriconi, G. (2006), "Behavior of beam-column joints made of sustainable concrete under cyclic loading", *J. Mater. Civil Eng.*, **18**(5), 650-658.

Corinaldesi, V., Letelier, V. and Moriconi, G. (2011), "Behavior of beam-column joints made of recycled-aggregate concrete under cyclic loading", *Constr. Build. Mater.*, **2**, 1877-1882.

Dhaval, K., Scott, R.H., Deb, S.K. and Dutta, A. (2015), "Ductility enhancement in beam-column connections using hybrid fiber-reinforced concrete", *ACI Struct. J.*, **112**(2), 167-178.

Foti, D. (2011), "Preliminary analysis of concrete reinforced with waste bottles PET fibers", *Constr. Build. Mater.*, **25**(4), 1906-1915.

Foti, D. (2013), "Use of recycled waste pet bottle fibers for the reinforcement of concrete", *Compos. Struct.*, **96**, 396-404.

Fraternali, F., Ciancia, V., Chechile, R., Rizzano, G., Feo, L. and Incarnato, L. (2011), "Experimental study of the thermo-mechanical properties of recycled PET fiber reinforced concrete", *Compos. Struct.*, **93**, 2368-2374.

Fraternali, F., Farina, I., Polzone, C., Pagliuca, E. and Feo, L. (2013), "On the use of R-PET strips for the reinforcement of cement mortars", *Compos. Part B, Eng.*, **46**, 207-210.

Ghobarah, A. and Said, A. (2002), "Shear strengthening of beam-column joints", *Eng. Struct.*, **24**(7), 881-888.

Ghobarah, A., Aziz, A. and Biddah, T.S. (1997), "Rehabilitation of reinforced concrete frame connections using corrugated steel jacketing", *ACI Struct. J.*, **4**(3), 283-294.

Hadi, N.S. and Tran, T.M. (2014), "Retrofitting non-seismically detailed exterior beam-column joints using concrete covers together with CFRP jacket", *Constr. Build. Mater.*, **63**, 161-173.

Han, B.C., Yun, H.D. and Chung, S.Y. (2001), "Shear capacity of reinforced concrete beams made with recycled aggregate", *ACI Spec. Publ.*, **200**, 503-516

Hansen, T.C. (1992), *Recycling of Demolished Concrete and Masonry*, Taylor and Francis, Oxfordshire, UK.

IS 10262 (2009), Guidelines for Concrete Mix Design Proportioning (CED 2: Cement and Concrete), Bureau of Indian Standard New Delhi.

IS 1199 (1959), Methods of Sampling and Analysis of Concrete, Bureau of Indian Standard New Delhi.

IS 12269 (1987), Specification for OPC-53 Grade Cement, Bureau of Indian Standard New Delhi.

IS 13920 (1993), Ductile Detailing of Reinforced Concrete Structures Subjected to Seismic Forces-Code of Practice, Bureau of Indian Standard New Delhi.

IS 1608 (1995), Mechanical Testing of Metals-Tensile Testing, Bureau of Indian Standard New Delhi.

IS 2386a (1963), Methods of Test for Aggregates for Concrete-Part 1: Particle Size and Shape, Bureau of Indian Standard New Delhi.

IS 2386b (1963), Methods of Test for Aggregates for Concrete-Part 3: Specific Gravity, Density, Voids, Absorption and Bulking, Bureau of Indian Standard New Delhi.

IS 432 (1) (1982), Specification for Mild Steel and Medium Tensile Steel Bars and Hard-Drawn Steel Wire for Concrete Reinforcement: Part I Mild Steel and Medium Tensile Steel Bars, Bureau of Indian Standard New Delhi.

IS 456 (2000), Plain and Reinforced Concrete-Code of Practice, Bureau of Indian Standard New Delhi.

IS 519 (1959), Method of Tests for Strength of Concrete, Bureau of Indian Standard New Delhi.

IS 5816 (1999), Method of Test Splitting Tensile Strength, Bureau of Indian Standard New Delhi.

Jo, B., Park, S. and Park, J. (2008), "Mechanical properties of polymer concrete made with recycled PET and recycled concrete aggregates", *Constr. build. Mater.*, **22**, 2281-2291.

Karayannis, C.G. and Sirkelis, G.M. (2008), "Strengthening and rehabilitation of RC beam-column joints using carbon-FRP jacketing and epoxy resin injection", *J. Earthq. Eng. Struct. Dyn.*, **37**, 769-790.

Karayannis, C.G., Chalioris, C.E. and Sirkelis, G.M. (2008), "Local retrofit of exterior beam-column joints using thin RC jackets-An experimental study", *Earthq. Eng. Struct. Dyn.*, **37**, 727-746.

Kim, S.B., Yi, N.H., Kim, H.Y., Kim-Jay, H.J. and Song, Y.C. (2010), "Material and structural performance evaluation of recycled PET fiber reinforced concrete", *Cement Concrete Compos.*, **32**, 232-240.

Kong, D., Lei, T., Zheng, J., Ma, C. and Jiang, J. (2010), "Effect and mechanism of surfacecoating pozzalanics materials around aggregate on properties and ITZ microstructure of recycled aggregate concrete", *Constr. Build. Mater.*, **24**, 701-708.

Kou, S.C., Poon, C.S. and Chan, D. (2007), "Influence of fly ash as cement replacement on the properties of recycled aggregate concrete", *J. Mater. Civil Eng.*, **19**(9), 709-717.

Kumar, V., Nautiyal, B.D. and Kumar, S. (1991), "A study of exterior beam-column joints", *Ind. Concrete J.*, **65**(1), 39-43.

Limbachiya, M.C., Koulouris, A., Roberts, J.J. and Fried, A.N. (2004), "Performance of recycled aggregate concrete", *RILEM International Symposium on Environment Conscious Materials and System for Sustainable Development*, 127-136.

Marthong, C. (2015), "Effects of PET fiber arrangement and dimensions on mechanical properties of concrete", *IES J. Part A: Civil Struct. Eng.*, **8**(2), 111- 120.

Marthong, C. and Marthong, S. (2015), "Enhancing mechanical properties of concrete prepared with coarse recycled aggregates", *IES J. Part A: Civil Struct. Eng.*, **8**(3), 175-183.

Marthong, C. and Marthong, S. (2016), "An experimental study on the effect of PET fibers on the behavior of exterior RC beam-column connection subjected to reversed cyclic loading", *Struct.*, **5**, 175-185.

Marthong, C. and Sarma, D.K. (2015), "Influence of PET fiber

geometry on the mechanical properties of concrete: An experimental investigation", *Eur. J. Environ. Civil Eng.*, **20**(7), 771-784.

Marthong, C., Dutta, A. and Deb, S.K. (2013), "Seismic rehabilitation of RC exterior beam-column connections using epoxy resin injection", *J. Earthq. Eng.*, **17**(3), 378-398.

Matheus, F.A.S. and Vladimir, G.H. (2016), "Parametrical study of the behavior of exterior unreinforced concrete beam-column joints through numerical modeling", *Comput. Concrete*, **18**(2), 215-233

Naeim, F. and Kelly, J.M. (1999), *Design of Seismic Isolated Structures from Theory to Practice*, John Willey & Sons, Inc.

Oinam, R.M., Sahoo, D.R. and Sindhu, R. (2014), "Cyclic response of non-ductile RC frame with steel fibers at beam-column joints and plastic hinge regions", *J. Earthq. Eng.*, **18**(6), 908-928.

Padmini, A.K., Ramamurthy, K. and Mathews, M.S. (2009), "Influence of parent concrete on the properties of recycled aggregate concrete", *Constr. Build. Mater.*, **23**, 829-836.

Panyakapo, P. and Panyakapo, M. (2007), "Reuse of thermosetting plastic waste for lightweight concrete", *Waste Manage.*, **28**, 1581-1588.

Park, Y.J. and Ang, A.H.S. (1985), "Mechanistic seismic damage model for reinforced concrete", *J. Struct. Eng.*, **111**(4), 722-739.

Pereira de Oliveira, L.A. and Castro-Gomes, J.P. (2011), "Physical and mechanical behavior of recycled PET fiber reinforced mortar", *Constr. Build. Mater.*, **25**, 1712-1717.

Rao, M.C., Bhattacharyya, S.K. and Barai, S.V. (2011), "Influence of field recycled coarse aggregate on properties of concrete", *Mater. Struct.*, **44**, 205-20.

Sasmal, S., Ramanjaneyulu, K., Novak, B., Srinivas, V., Kumar, K.S., Korkowski, C., Roehm, C., Lakshmanan, N. and Iyer, N.R. (2010), "Seismic retrofitting of non ductile beam-column sub-assemblage uses FRP wrapping and steel plate jacketing", *Constr. Build. Mater.*, **25**(1), 175-182.

Shannag, M.J. and Alhassan, M.A. (2005), "Seismic upgrade of interior beam-column sub-assemblages with high performance fiber reinforced concrete jackets", *ACI Struct. J.*, **102**(1), 131-138.

Shannag, M.J. and Ziyyad, T.B. (2007), "Flexural response of ferrocement with fibrous cementitious matrices", *Constr. Build. Mater.*, **21**, 1198-1205.

Tabsh, S.W. and Abdelfatah, A.S. (2009), "Influence of recycled concrete aggregates on strength properties of concrete", *Constr. Build. Mater.*, **23**, 1163-1167.

Vidjeapriya, R. and Jaya, K.P. (2013), "Experimental study on two simple mechanical precast beam-column connections under reverse cyclic loading", *J. Perform. Constr. Facil.*, **27**(4), 402-414.

Viviana, C., Gonzalez, L. and Moriconi, G. (2014), "The influence of recycled concrete aggregates on the behavior of beam-column joints under cyclic loading", *Eng. Struct.*, **60**, 148-154.

Xiao, J., Sun, Y. and Falkner, H. (2006), "Seismic performance of frame structures with recycled aggregate concrete", *Eng. Struct.*, **28**, 1-8.

Xiao, J.Z., Li, W., Fan, Y. and Huang, X. (2012), "An overview of study on recycled aggregate concrete in China (1996-2011)", *Constr. Build. Mater.*, **31**, 364-83.

HK